AMERICAN SOCIETY FOR MICROBIOLOGY | Molecular and Cellular Biology®

RESEARCH ARTICLE

Reduction of Cellular Nucleic Acid Binding Protein Encoded by a Myotonic Dystrophy Type 2 Gene Causes Muscle Atrophy

Christina Wei,[a]* Lauren Stock,[a] Christiane Schneider-Gold,[b] Claudia Sommer,[c] Nikolai A. Timchenko,[d] Lubov Timchenko[a]

[a]Division of Neurology, Cincinnati Children's Hospital Medical Center, Cincinnati, Ohio, USA
[b]Department of Neurology, St. Josef Hospital, Ruhr University Bochum, Bochum, Germany
[c]Department of Neurology, University of Würzburg, Würzburg, Germany
[d]Division of Surgery, Cincinnati Children's Hospital Medical Center, Cincinnati, Ohio, USA

ABSTRACT Myotonic dystrophy type 2 (DM2) is a neuromuscular disease caused by an expansion of intronic CCTG repeats in the *CNBP* gene, which encodes a protein regulating translation and transcription. To better understand the role of cellular nucleic acid binding protein (CNBP) in DM2 pathology, we examined skeletal muscle in a new model of *Cnbp* knockout (KO) mice. This study showed that a loss of Cnbp disturbs myofibrillar sarcomeric organization at birth. Surviving homozygous *Cnbp* KO mice develop muscle atrophy at a young age. The skeletal muscle phenotype in heterozygous *Cnbp* KO mice was milder, but they developed severe muscle wasting at an advanced age. Several proteins that control global translation and muscle contraction are altered in muscle of *Cnbp* KO mice. A search for CNBP binding proteins showed that CNBP interacts with the α subunit of the dystroglycan complex, a core component of the multimeric dystrophin-glycoprotein complex, which regulates membrane stability. Whereas CNBP is reduced in cytoplasm of DM2 human fibers, it is a predominantly membrane protein in DM2 fibers, and its interaction with α-dystroglycan is increased in DM2. These findings suggest that alterations of CNBP in DM2 might cause muscle atrophy via CNBP-mediated translation and via protein-protein interactions affecting myofiber membrane function.

KEYWORDS CNBP, myotonic dystrophy, molecular pathology, muscle atrophy, unstable repeats

Myotonic dystrophy type 2 (DM2) is a multisystem disease characterized by muscle weakness and atrophy, myotonia, cardiac involvement, impairment of central nervous system (CNS) function, insulin resistance, cataracts, hypogonadism, and daytime sleepiness (1). DM2 is caused by an expansion of unstable CCTG repeats in intron 1 of the gene encoding cellular nucleic acid binding protein (CNBP) (also known as zinc finger factor 9 [ZNF9]) (2). The DM2 phenotype is similar to that of myotonic dystrophy type 1 (DM1), a multisystem neuromuscular disease caused by unstable CTG repeats in the 3′ untranslated region (UTR) of the *DMPK* gene (3). However, DM2 pathology affects mainly proximal muscles, whereas DM1 affects distal muscles (1, 4). In both DM1 and DM2, mutant transcripts accumulate in patients' cells, misregulating RNA metabolism via specific RNA binding proteins (5, 6).

CNBP possesses DNA and RNA binding activities and may regulate transcription and cap-dependent and cap-independent translation (7). CNBP binds to the 5′ UTRs of mRNAs containing a terminal oligopyrimidine tract (TOP), which encode proteins controlling global translation: ribosomal proteins (such as RPS17), eukaryotic elongation factors (eEF1/2), and RNA binding proteins controlling translation [such as the poly(A) binding protein PABPC1] (8, 9). The translation of the TOP-containing mRNAs (TOP-mRNAs) requires fine control during stress to quickly repress translation to preserve energy and reactivate translation during stress recovery. A recent study

Received 15 December 2017 **Returned for modification** 10 January 2018 **Accepted** 26 April 2018

Accepted manuscript posted online 7 May 2018

Citation Wei C, Stock L, Schneider-Gold C, Sommer C, Timchenko NA, Timchenko L. 2018. Reduction of cellular nucleic acid binding protein encoded by a myotonic dystrophy type 2 gene causes muscle atrophy. Mol Cell Biol 38:e00649-17. https://doi.org/10.1128/MCB.00649-17.

Address correspondence to Lubov Timchenko, Lubov.Timchenko@cchmc.org.

* Present address: Christina Wei, Merck Research Laboratories, West Point, Pennsylvania, USA.

connected CNBP function to repression of translation in response to stress (10). In agreement, CNBP binds to multiple mRNAs, regulating their translation (11).

The ability of CNBP to regulate RNA processing at the level of translation suggests that misregulation of CNBP in DM2 tissues might contribute to the abnormal RNA metabolism. Examination of a single model of *Cnbp* knockout (KO) mice showed that a loss of Cnbp is lethal and that heterozygous mice develop skeletal and cardiac muscle abnormalities similar to those in patients with DM2 (12). Later studies revealed that CNBP is reduced in DM2 muscle biopsy specimens and in DM2 muscle precursors (8, 13, 14). However, other studies found no changes of CNBP in DM2 (15–17).

We have previously shown that CNBP is reduced in cytoplasm of DM2 biopsied muscle and that proteins encoded by the TOP-mRNAs (RPS17, PABPC1, and eEF1/2) were also reduced in DM2 muscle (8). These findings suggested that the cytoplasmic reduction of CNBP in DM2 might cause muscle atrophy through reduction of synthesis of muscle proteins. In addition to the TOP-containing mRNAs, human CNBP or its yeast ortholog Gis has putative binding sites in mRNAs encoding major muscle proteins and their regulators (18). Therefore, the reduction of CNBP in DM2 might cause misregulation of expression of major muscle proteins, leading to muscle weakness.

To better understand the role of CNBP in DM2, we examined the effect of Cnbp deletion on skeletal muscle structure during the mouse life span and found that a reduction of Cnbp causes severe muscle atrophy in old mice, whereas loss of Cnbp leads to muscle atrophy at a young age. We also examined the CNBP intracellular distribution in human myofibers and searched for protein partners of CNBP. These studies confirmed a reduction of cytoplasmic CNBP in DM2 human muscle sections and showed that CNBP is located mainly in DM2 fiber membrane. We found that in skeletal muscle, CNBP interacts with α-dystroglycan (α-DG), which binds through β-dystroglycan with the dystrophin-associated protein complex (DAPC). These findings suggest that alterations of CNBP in DM2 might cause muscle atrophy not only via misregulation of mRNA but also via protein-protein interactions with membrane proteins.

RESULTS

Generation of *Cnbp* KO mice. A previous study showed that the deletion of Cnbp in mice affects development, causing the embryonic lethality of homozygous (hom) *Cnbp* KO mice (19). Although examination of heterozygous (het) mice in a following study (12) suggested that a reduction of Cnbp causes multitissue abnormalities, including muscle wasting and weakness, the muscle loss in *Cnbp* KO mice was not quantified. In addition, the muscle histopathology was analyzed only in adult, 2- to 6-month-old het *Cnbp* KO mice. Since DM2 usually affects patients in their 60s, examination of skeletal muscle in older mice is important to determine if a reduction of CNBP in human patients contributes to the worsening of muscle atrophy with age. To address these questions, we generated *Cnbp* KO mice using a gene trap approach (Fig. 1A and B). Insertion of the trap vector disrupted expression of Cnbp protein. We found that the levels of Cnbp were ~2-fold reduced in skeletal muscle of het *Cnbp* KO mice and that Cnbp was undetectable by Western blotting assay in hom *Cnbp* KO mice (Fig. 1C to G). The reduction of Cnbp in het *Cnbp* KO mice was observed with two types of antibodies (Abs), i.e., affinity-purified rabbit antibodies, previously developed in our lab (8) and commercial goat antibodies (Fig. 1C and E). Cnbp was reduced not only in skeletal muscle of het *Cnbp* KO mice but also in heart (Fig. 1F and G). Thus, we conclude that the expression of Cnbp is not detectable in hom *Cnbp* KO mice and is approximately 2-fold reduced in het *Cnbp* KO mice.

Gross analysis of *Cnbp* KO mice showed that the deletion of Cnbp interferes with normal development (Fig. 2A). For that reason, *Cnbp* KO mice were maintained as heterozygous. The breeding of het *Cnbp* KO females and het males produced 47 litters with an average size of 6.6 pups per litter. In contrast to the previous study (12), approximately 43.6% of expected hom *Cnbp* KO mice in our colony were born, and a portion of them survived until 16 to 20 months of age (Fig. 2B). The difference between the two mouse strains cannot be due to minor expression of Cnbp in our strain,

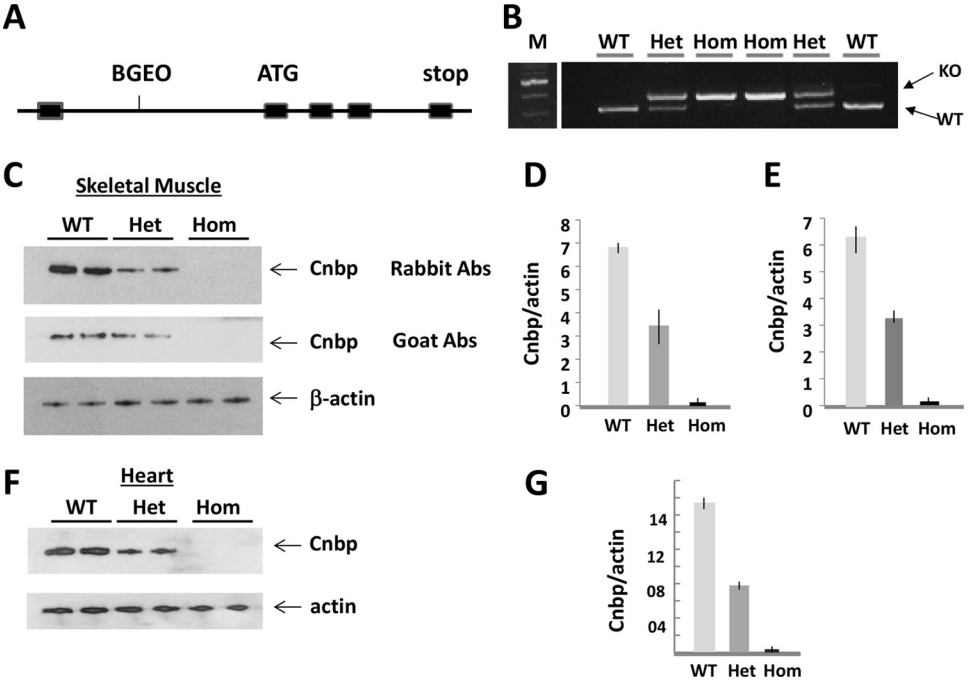

FIG 1 Generation of *Cnbp* KO mice. (A) Location of an intronic insertion of the trap vector, containing *βgeo* (a fusion of *lacZ* and *neo*) in front of ATG codon of the *Cnbp* gene. *βgeo* generates *β*-galactosidase and provides resistance to neomycin. (B) Example of genotyping of *Cnbp* KO mice. M, DNA markers. WT and mutant bands are shown by the arrows. (C) Western blot analysis of whole-cell extracts from skeletal muscle samples (gastrocnemius) from 3- to 4-month-old WT, het, and hom *Cnbp* KO mice (all males) with two antibodies: affinity-purified rabbit anti-peptide CNBP (8) and goat anti-CNBP from Abcam. *β*-Actin was used as a control for loading. (D and E) Quantification of Cnbp signals as ratios to *β*-actin in panel C obtained with rabbit (D) and goat (E) antibodies. (F) Western blot analysis of Cnbp from whole-cell protein extracts from cardiac muscle of 3- to 4-month-old WT, het, and hom *Cnbp* KO mice with affinity purified rabbit anti-CNBP antibodies and *β*-actin as a control. (G) Quantification of Cnbp signals shown in panel F.

because Cnbp was not detectable in tissues of our mice (Fig. 1C to G). The difference also cannot be explained by possible disruption of additional genes in the previous strain, because crossing of *Cnbp* KO with *Cnbp* transgenic mice corrected the phenotype in *Cnbp* KO mice (12). We suggest that the milder phenotype in our strain could be due to differences in genetic background. Whereas our mice were generated on a pure C57BL background, the mice in the previous study were generated using pseudopregnant foster mothers on a mixed C57BL/6J × CBA background (19). The increased rate of homozygous survivors in our strain could be also due to careful monitoring of *Cnbp* KO mice during the postnatal period. We noticed that whereas some small newborn pups died shortly after birth, others could survive despite their small size and delayed development when kept with foster mothers until 2 to 3 months of age.

hom *Cnbp* KO mice were smaller than wild-type (WT) littermates, and they remained smaller during their life span (Fig. 2A, C, and D). Approximately 12% of surviving hom *Cnbp* KO mice were very weak and died during the first month. het *Cnbp* KO mice of both genders steadily gained weight from 1 to 12 months, with a minor reduction of body weight at 12 months in het females and at 6 months in het males (Fig. 2C and D). However, hom *Cnbp* KO mice (males and females) were significantly smaller at all ages examined (1, 3, 6, and 12 months). There was a delay of development of hom *Cnbp* KO males and females during 3 to 6 months as judged by the lack of body weight gain during this period (Fig. 2C and D). The significant reduction of the body weight of hom *Cnbp* KO mice and almost normal weight of het mice show that the delay of development and growth is dependent on the Cnbp dose.

Loss of Cnbp disturbs the sarcomeric structure in neonatal skeletal muscle. Several reports showed that CNBP is reduced (but not completely lost) in muscle biopsy

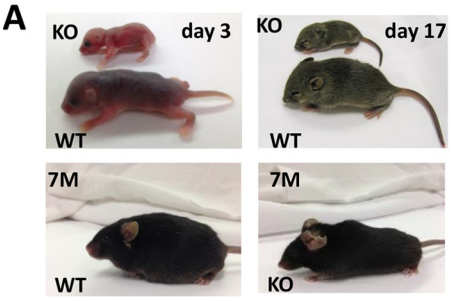

B

	Expected mice	Born mice	Wean
WT	78	94	92
Het Cnbp KO	156	184	179
Hom *Cnbp* KO	78	34	30
P-value	2.27E-05		

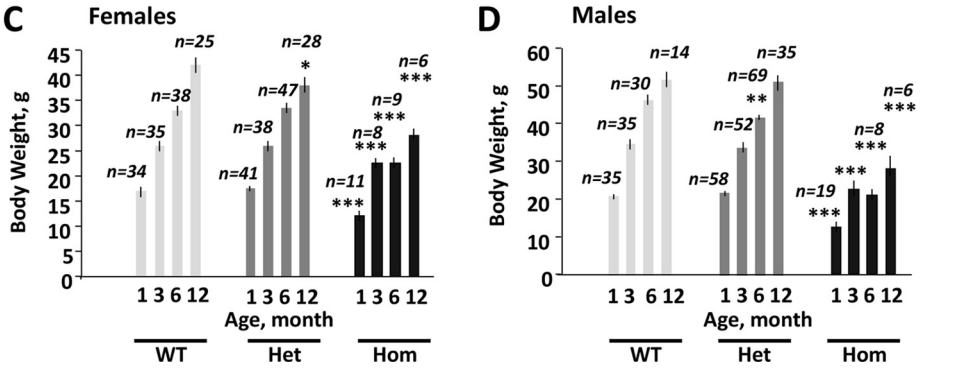

FIG 2 Effect of deletion of Cnbp on development and growth. (A) Top panels, WT and hom *Cnbp* KO littermates at 3 and 17 days of age. Bottom, the 7-month-old hom *Cnbp* KO mice have abnormal posture, likely due to muscle weakness. (B) Deletion of *Cnbp* interferes with development, reducing the number of hom *Cnbp* KO mice. The *P* value is 2.27E−05, determined by Fisher's test. (C and D) Body weights of *Cnbp* KO females (C) and males (D) at different ages. The numbers of examined mice are shown above the bars. *, $P < 0.05$; **, $P < 0.01$; ***, $P < 0.001$ (for WT versus mutant mice).

specimens from patients with DM2 (8, 13, 14). Therefore, we focused mainly on the examination of skeletal muscle in *Cnbp* KO mice. Since many hom *Cnbp* KO mice die at birth, we analyzed the effect of Cnbp loss on skeletal muscle morphology in neonatal mice. The hematoxylin and eosin (H&E) staining of transverse and longitudinal sections of the hind limbs of 4-day-old WT and *Cnbp* KO mice showed that the neonatal skeletal muscle in hom *Cnbp* KO mice contains small and thin fibers (Fig. 3A and B). Some fibers in postnatal hom *Cnbp* KO muscle contain centralized nuclei.

Previous reports showed that CNBP is associated with sarcomeres (14, 17). Therefore, we examined whether the loss of Cnbp affects the sarcomeric structure. The hind-limb muscles of 1-day-old WT and hom *Cnbp* KO mice were examined by electron microscopy (EM) (Fig. 3C to G). This analysis showed that the number of myofibrils and the number of sarcomeres were significantly reduced in neonatal muscle of hom *Cnbp* KO mice (Fig. 3D and E). Sarcomeres were shorter in neonatal hom *Cnbp* KO muscle, and some of them were disorganized (Fig. 3C and F). Approximately half of sarcomeres in 1-day-old hom *Cnbp* KO muscle contained disrupted I bands (Fig. 3G). The sarcomere length might be changed in DM2 muscle because of the presence of myotonia. However, disruption of the I bands in the sarcomeres of *Cnbp* KO muscle suggests that the sarcomeric structure is affected by the deletion of Cnbp. Since CNBP is located in the I bands in human muscle (17), the lack of Cnbp in hom *Cnbp* KO mice possibly leads to the disorganization of I bands and significant disruption of the sarcomeric structure in neonatal skeletal muscle.

Loss of Cnbp causes muscle atrophy at young age, whereas a reduction of Cnbp causes muscle loss at advanced age. We previously found that the rate of protein synthesis is reduced in DM2 myoblasts, possibly due to a reduction of cytoplasmic ZNF9/CNBP (8). It was expected that the reduction of the rate of protein synthesis in *Cnbp* KO mice leads to muscle wasting. To examine whether the deficit of Cnbp causes muscle atrophy, we analyzed skeletal muscle histology in *Cnbp* KO mice

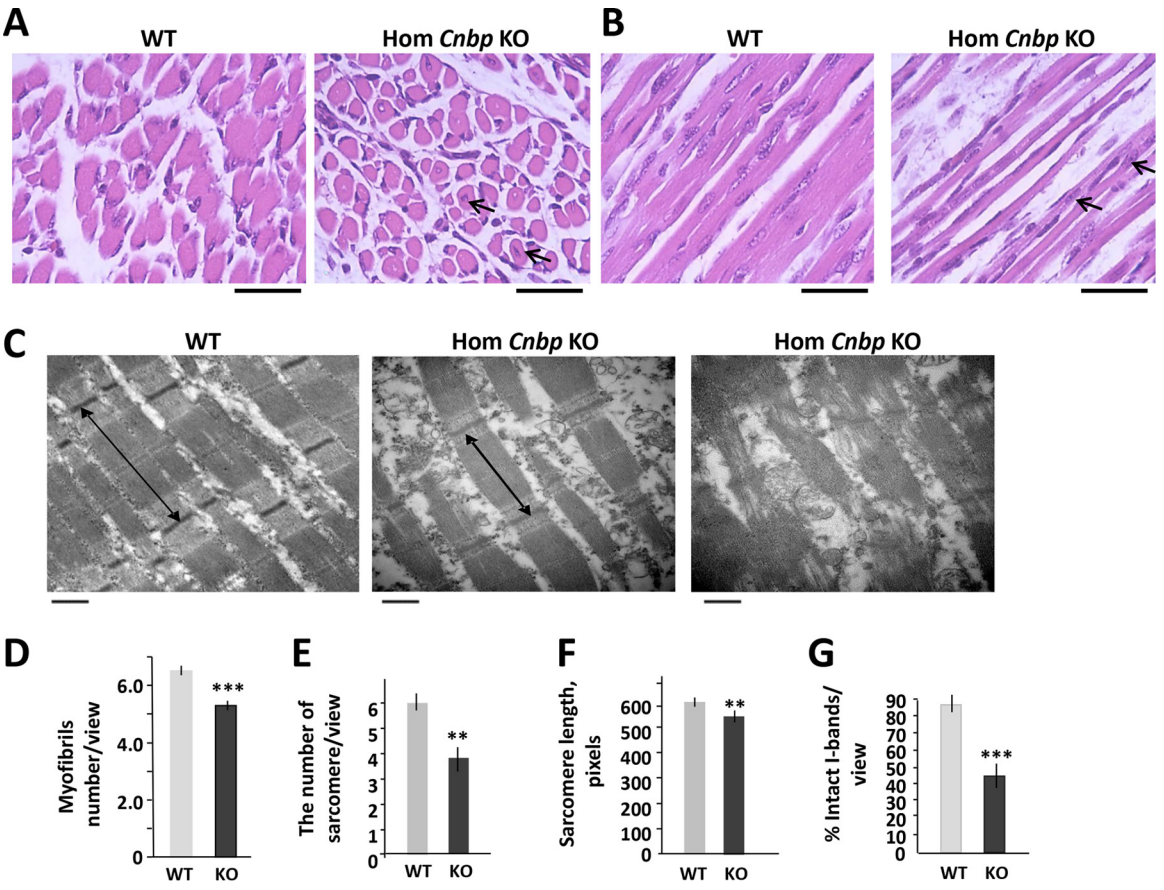

FIG 3 Deletion of *Cnbp* affects sarcomeric structure in neonatal mice. (A and B) H&E analysis of transverse (A) and longitudinal (B) sections of the hind-limb muscles of 4-day-old WT and hom *Cnbp* KO mice. Arrows point to fibers with centralized nuclei. Scale bars, 20 μm. (C) EM images of hind-limb muscle of 1-day-old WT and hom *Cnbp* KO mice. Scale bars, 500 nm. Sarcomeres are shown by arrows. Two EM images of skeletal muscle from hom *Cnbp* KO mice demonstrate sarcomeres with different degrees of disruption. (D to G) Average myofibril number (D), sarcomere number (E), average length of sarcomeres (F), and percentage of intact I bands (G) in skeletal muscle of 1-day-old WT and hom *Cnbp* KO mice per view at a magnification of $\times$30,000. **, $P < 0.01$; ***, $P < 0.001$ (for WT versus mutant mice).

at different ages. H&E analysis showed that skeletal muscle in young hom *Cnbp* KO mice is characterized by general fiber atrophy (Fig. 4A). The average fiber area is significantly reduced in muscle of 1-month-old hom *Cnbp* KO mice but not in matched het mice (Fig. 4A and B).

Skeletal muscle in 1-month-old hom *Cnbp* KO muscle contains small atrophic fibers, pyknotic nuclei (which are often observed in patients with DM2), and hyaline fibers (Fig. 4A). These histological findings suggest that general fiber atrophy in muscle of hom *Cnbp* KO mice at a young age is not due to a delay in development but is associated with muscle pathology. The presence of small angulated fibers and pyknotic nuclei/pyknotic nuclear clumps in hom *Cnbp* KO muscle indicate a neurogenic component of muscle damage, which is frequently found in human DM2 biopsy specimens (20). The H&E analysis of the fiber size in muscle of young het *Cnbp* KO mice showed a variability of myofiber size with the presence of some angulated atrophic fibers (data not shown). A variability of myofiber size is one of the features of muscle pathology in DM1 and in DM2. A variability of myofiber size in muscle of het *Cnbp* KO mice at a young age shows that a partial loss of CNBP in DM2 is sufficient to lead to muscle pathology.

The presence of many small, atrophic fibers in muscle of young hom *Cnbp* KO mice suggests that the loss of Cnbp might cause muscle atrophy at a young age. To address this issue, we compared the weight of the gastrocnemius muscle (gastroc) relative to body weight in 1-month-old WT, het, and hom *Cnbp* KO mice. This analysis showed that the gastroc weight was almost normal in 1-month-old het *Cnbp* KO mice; however, the

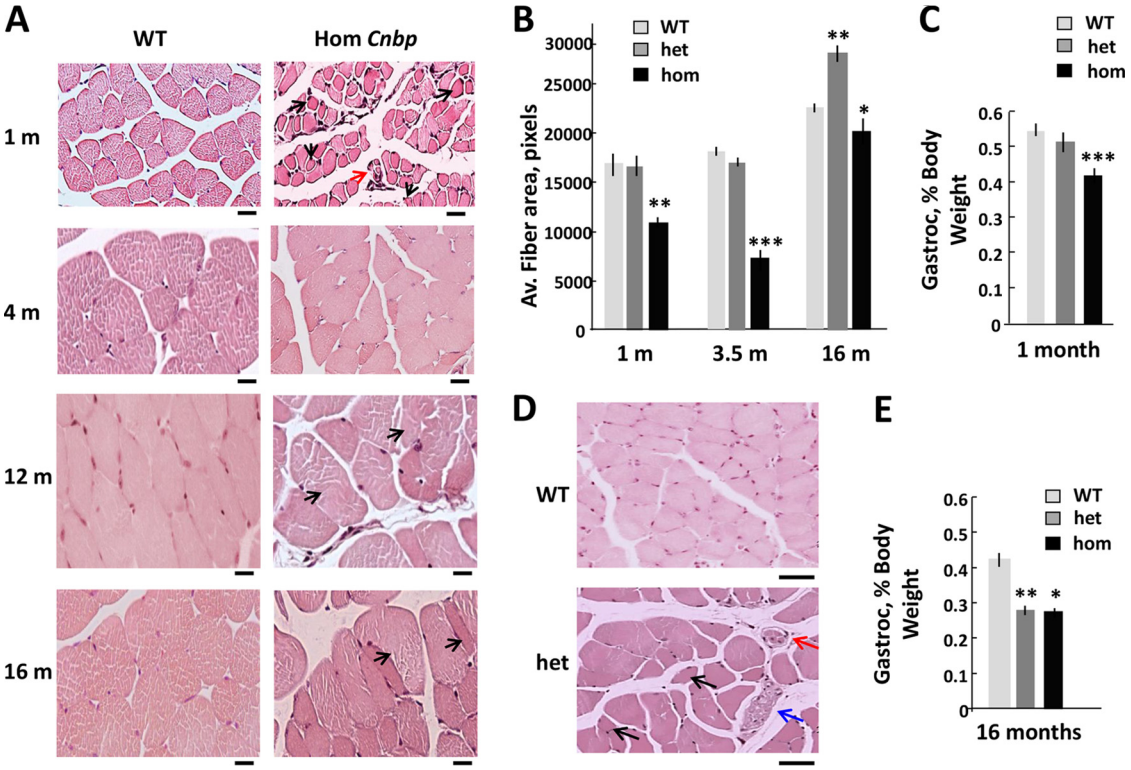

FIG 4 Muscle atrophy in young hom and old het *Cnbp* KO mice. (A) H&E staining of gastroc of 1-month-, 4-month-, 12-month-, and 16-month-old WT and hom *Cnbp* KO mice (males). Note the generalized fiber atrophy in 1-month-old hom *Cnbp* KO mice. Markedly atrophic and hyaline fibers are shown by black arrows. A group of very small atrophic fibers appears as nuclear clumps (red arrow). Note the fiber size variability in 4-, 12-, and 16-month-old hom *Cnbp* KO mice. Fibers with very large and small areas in muscle of 12- and 16-month-old hom *Cnbp* KO mice are shown by arrows. Scale bars, 15 μm. (B) Average fiber area in cross sections of gastroc from 1-month, 3.5-month, and 16-month-old WT, het, and hom *Cnbp* KO mice. Three mice per group were analyzed in 1- and 3.5-month-old groups of WT, het, and hom mice. The 16-month-old group contained 3 WT, 3 het, and 2 hom mice. Only two 16-month-old hom *Cnbp* males were available, whereas a few hom females lived until approximately 20 months. The *P* values in the 1-month-old group were <0.01 by ANOVA and <0.01 for WT versus hom mice and for het versus hom mice by the Student *t* test. In the 3.5-month group, the *P* values were <0.0001 by ANOVA and <0.01 for het versus hom mice and <0.001 for WT versus hom mice by the Student *t* test. In the 16-month group, the *P* values were <0.01 by ANOVA and <0.05 and 0.01 for WT versus hom and WT versus het mice, respectively, by the Student *t* test. (C) Percentage of gastroc weight relative to body weight in 1-month-old WT ($n = 3$), het ($n = 4$), and hom ($n = 3$) *Cnbp* KO mice (all males). The *P* values were <0.01 by ANOVA and <0.001 for WT versus hom mice by the Student *t* test. Sample standard deviations are shown. (D) H&E staining of soleus from the matched 18.5-month-old WT and het *Cnbp* KO mice. Scale bars, 20 μm. The images show normal fibers in WT muscle and increased fiber size variability with small atrophic fibers (black arrows) in het *Cnbp* KO mice. A basophilic degenerating fiber (blue arrow) and a muscle spindle (red arrow) can be seen in muscle of old het *Cnbp* KO mice. (E) Percentage of gastroc weight relative to the body weight in 16-month-old WT ($n = 4$), het ($n = 4$), and hom ($n = 2$) *Cnbp* KO mice. The *P* values were <0.01 between groups by ANOVA and <0.05 and <0.01 by the Student *t* tests for WT versus het and WT versus hom mice, respectively. Standard deviations are shown.

gastroc weight was significantly reduced in young hom *Cnbp* KO mice, to approximately 76% of that of WT littermates (Fig. 4C). Thus, the loss of Cnbp *in vivo* leads to a severe muscle wasting even at a young age, while the reduction of Cnbp in young het *Cnbp* KO mice does not result in muscle atrophy.

Patients with DM2 develop pathology at old age (1, 6). Therefore, we examined muscle histology in adult and old het and hom *Cnbp* KO mice. H&E analysis showed the presence of small atrophic fibers and variability of fiber size in 4-, 12-, and 16-month-old hom *Cnbp* KO mice (Fig. 4A). Examination of the average fiber area in 4- and 16-month-old hom *Cnbp* KO mice showed that the fiber size in adult and old hom mice remains reduced (Fig. 4A and B).

The average myofiber area was normal in adult (4-month) het *Cnbp* KO muscle (Fig. 4B). However, the average cross-sectional fiber area was significantly increased in 16-month-old het *Cnbp* KO mice. The H&E analysis showed that the increase of the average fiber area in old het mice could be due to the increase of very large,

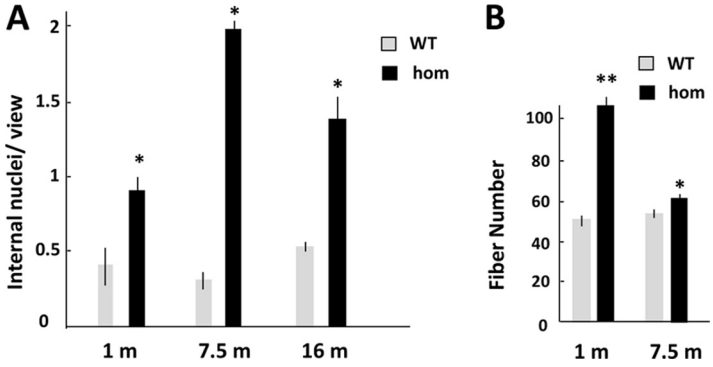

FIG 5 (A) Average number of centralized nuclei per view at a magnification of ×20 in gastroc of gender-matched (male) 1-month-old WT ($n = 3$) and hom *Cnbp* KO ($n = 3$) mice, 7.5-month-old WT ($n = 3$) and hom ($n = 3$) mice, and 16-month-old WT ($n = 3$) and hom ($n = 2$) mice. (B) Average fiber number in gastroc of 1- and 7.5-month-old WT and hom *Cnbp* KO mice. Three mice per group were analyzed. *, $P < 0.05$; **, $P < 0.01$ (for WT versus *Cnbp* KO mice).

hypertrophic fibers, including degenerated fibers (Fig. 4D). Muscle in old het *Cnbp* KO mice also contains small fibers, which likely represent atrophic fibers (Fig. 4D). We identified severe muscle wasting in old *Cnbp* KO mice of both genotypes. As shown in Fig. 4E, the gastroc weight, determined as a percentage of the body weight, was significantly reduced in 16-month-old het and hom *Cnbp* KO mice. The muscle wasting in old *Cnbp* KO mice of both genotypes is likely associated with the accumulation of atrophic, angulated fibers (Fig. 4A and D).

Myofibers in patients with DM2 accumulate central nuclei. The H&E staining showed that the number of central nuclei was increased in muscle of hom *Cnbp* KO mice (Fig. 5A). The appearance of central nuclei in fibers in these mice was associated with a significantly increased number of fibers, especially at a young age (Fig. 5B).

The accumulation of small atrophic fibers in muscle of *Cnbp* KO mice was accompanied by grip weakness. het *Cnbp* KO mice of both genders had significantly reduced grip strength during their life span (1, 3, 6, and 12 months) (Fig. 6A and B). We found that hom *Cnbp* KO mice were much weaker than het littermates.

It is known that muscle wasting in DM1 and DM2 may occur due to muscle loss alone or in combination with fat accumulation. We found that the total body fat was increased and lean mass was reduced in het *Cnbp* KO mice (Fig. 6C to F). These findings suggest that metabolism is changed in *Cnbp* KO mice. Additional studies are needed to determine whether Cnbp plays a role in the regulation of metabolism.

Based on the studies described above, we conclude that the loss of Cnbp in hom survivors causes muscle atrophy characterized by the accumulation of very small and atrophic fibers with central nuclei and a significant loss of muscle that begins at a young age. The muscle pathology in young and adult het *Cnbp* KO mice is mild and is characterized mainly by a significant variability of fiber size with the accumulation of small and enlarged fibers. Myofiber size variability progresses in het *Cnbp* KO mice during their life span, leading to severe muscle loss at an advanced age, possibly due to the increase of atrophic fibers.

Alteration of proteins encoded by TOP-containing mRNAs and proteins regulating muscle contraction in muscle of hom *Cnbp* KO mice. Previously, we showed that the TOP-containing mRNAs encoding ribosomal protein RPS17 and RNA binding protein PABPC1 are putative targets of CNBP and that RPS17 and PABPC1 are reduced in skeletal muscle biopsy specimens from patients with DM2 (8). To examine whether these proteins are altered in *Cnbp* KO mice, we analyzed protein levels of RPS17 and PABP1C1 in skeletal muscle of 3-month-old hom *Cnbp* KO mice and found that both proteins were decreased in hom *Cnbp* KO mice relative to those in matched WT mice (Fig. 7A and B). Thus, proteins encoded by the TOP-mRNAs are reduced in *Cnbp* muscle.

To identify additional proteins affected by the deletion of Cnbp, we examined proteins in muscle of hom *Cnbp* KO mice using two-dimensional (2D) gel separation

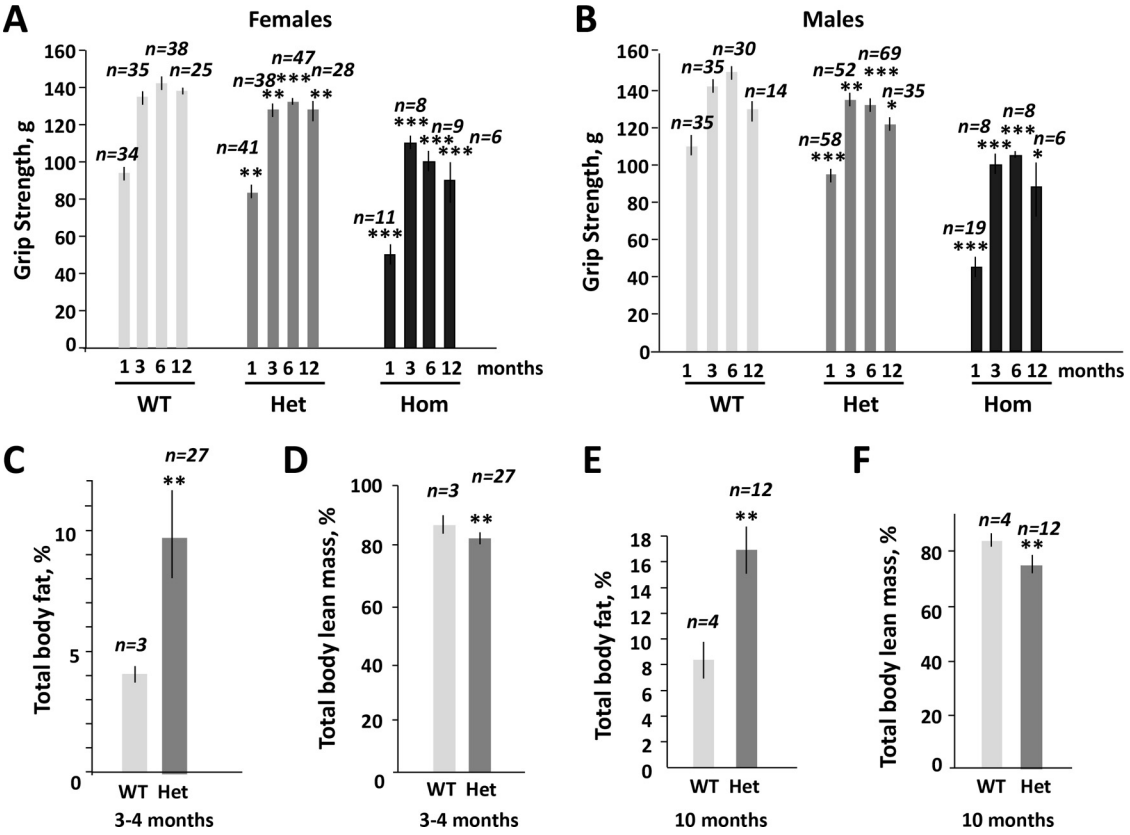

FIG 6 (A and B) Grip weakness in het and hom *Cnbp* KO females (A) and males (B) during their life span. (C to F) Increase of body fat and reduction of lean mass in het 3- to 4-month-old *Cnbp* KO males (C and D) and 10-month-old het females (E and F). The numbers of analyzed mice are shown above the bars. *, $P < 0.05$; **, $P < 0.01$; ***, $P < 0.001$ (for WT versus *Cnbp* KO mice).

and mass spectroscopy analysis. This analysis identified 79 protein spots with altered expression. Mass spectroscopy analysis of 10 well-separated spots identified 8 proteins with high confidence scores (100%) (Fig. 7C). These proteins include heat shock protein Hsp70, tropomyosin beta chain (TPM2), fast skeletal muscle troponin T (TNNT3), and skeletal muscle isoform of myosin regulatory light chain 2. In addition, phosphoglucomutase 1, carbonic anhydrase 3, dual-specificity protein phosphatase 3, and adenylate kinase were altered in *Cnbp* KO muscle. Cofilin 2 showed a reduction in *Cnbp* KO muscle, but the protein score was low due to a possible mix of this protein with other proteins in the 2D gel. Microphthalmia-associated transcription factor also showed a reduction in *Cnbp* KO muscle, but this protein spot was likely mixed with another large protein.

The increase of Hsp70 in muscle of hom *Cnbp* KO mice was expected because we previously observed the elevation of Hsp70 in DM2 myoblasts (21).

It has been shown that human and yeast CNBP proteins have predicted binding sites within mRNAs encoding skeletal muscle proteins involved in muscle contraction, such as myosins, utrophin, titin, triadin, laminin, dystrophin, TNNT3, and TPM2 (18). Some muscle mRNAs might contain multiple CNBP binding sites. For instance, mRNAs encoding TNNT3 and titin contain 28 and 30 to 50 predicted CNBP binding sites, respectively. Therefore, we expected alterations of proteins controlling the contractile apparatus in *Cnbp* KO muscle. Western blot analysis showed that TNNT3 and TPM2 are elevated in muscle of hom *Cnbp* KO mice (Fig. 7D and E). Thus, deletion of Cnbp in skeletal muscle leads to the alterations of proteins encoded by mRNAs containing predicted binding sites for Cnbp.

CNBP protein is reduced in cytoplasm of myofibers in human DM2 muscle biopsy specimens. The development of muscle atrophy and weakness in *Cnbp* KO

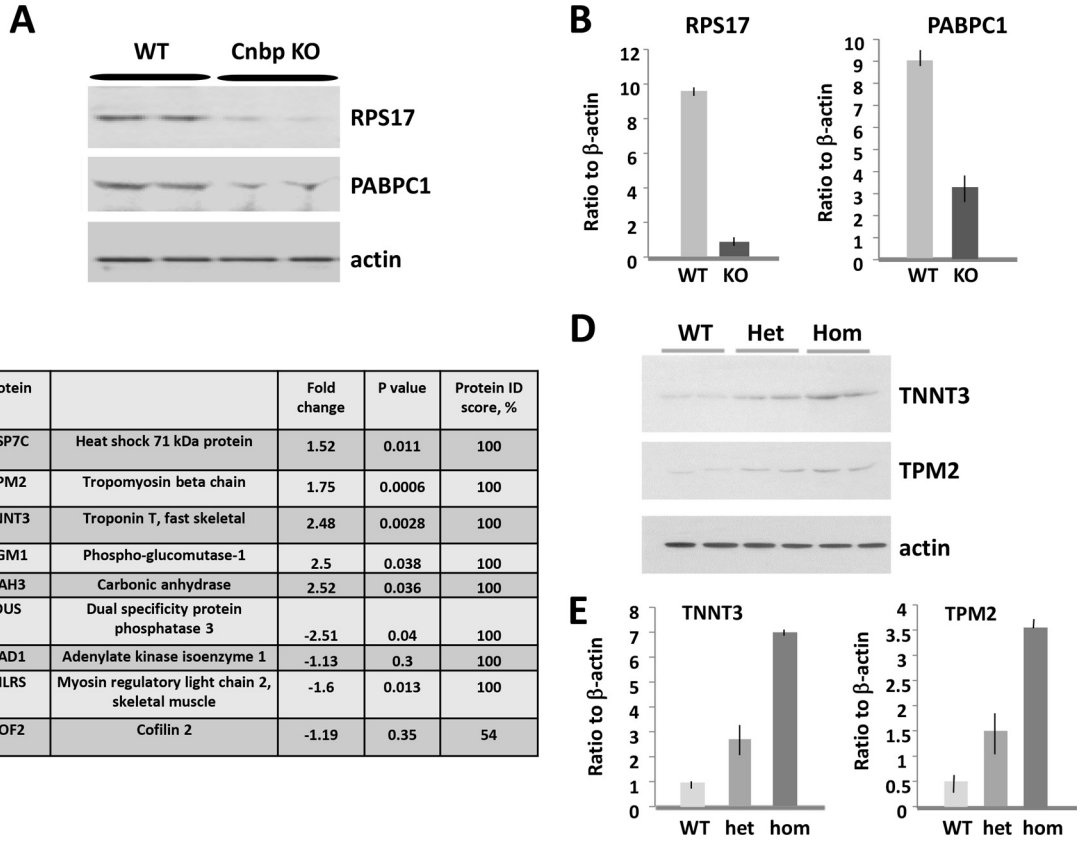

Protein		Fold change	P value	Protein ID score, %
HSP7C	Heat shock 71 kDa protein	1.52	0.011	100
TPM2	Tropomyosin beta chain	1.75	0.0006	100
TNNT3	Troponin T, fast skeletal	2.48	0.0028	100
PGM1	Phospho-glucomutase-1	2.5	0.038	100
CAH3	Carbonic anhydrase	2.52	0.036	100
DUS	Dual specificity protein phosphatase 3	-2.51	0.04	100
KAD1	Adenylate kinase isoenzyme 1	-1.13	0.3	100
MLRS	Myosin regulatory light chain 2, skeletal muscle	-1.6	0.013	100
COF2	Cofilin 2	-1.19	0.35	54

FIG 7 Disruption of TOP proteins and proteins involved in contractile function in skeletal muscle of *Cnbp* KO mice. (A) Western blot analysis of RPS17 and PABPC1 in gastroc of 2-month-old WT and hom *Cnbp* KO mice. Actin was used as a control. (B) Quantification of RSP17 and PABPC1 signals as a ratio to actin (shown in panel A). (C) Several proteins misregulated in soleus of hom *Cnbp* KO mice, identified by 2D separation and mass spectroscopy, include Hsp70 and proteins associated with contractile function. A protein score of 100% shows high confidence of sequence data, whereas a score below 100% shows low confidence due to a possible mix of proteins. (D) Western blot analysis of TNNT3 and TPM2 in gastroc of 2-month-old WT, het, and hom *Cnbp* KO littermates. β-Actin was used as a control. (E) Quantification of the TNNT3 and TPM2 signals shown in panel D.

mice demonstrated the significance of CNBP for the structure and function of skeletal muscle. Previously, we found a reduction of cytoplasmic CNBP/ZNF9 in human DM2 muscle biopsy specimens using Western blot analysis (8). However, the immunological analysis of CNBP in DM2 myofibers produced contradictory results in different labs (14, 17). Therefore, we examined CNBP expression in cross-sectional muscle from patients with DM2 using a quantitative immunofluorescence (IF) when the images were taken at the same brightness and time of exposure. This analysis showed that in normal human fibers, the CNBP signal is predominantly cytoplasmic, whereas in DM2 fibers, CNBP is reduced in cytoplasm and it is located predominantly in membrane (Fig. 8A). Thus, cytoplasmic CNBP is reduced in human DM2 myofibers, suggesting a reduction of cytoplasmic function of CNBP in patients with DM2.

IF analysis of skeletal muscle sections from WT and *Cnbp* KO muscle showed that Cnbp is localized in nuclei and in cytoplasm (Fig. 8B). Like in human muscle, the Cnbp signal was also detected in the membrane region.

CNBP protein interacts with α-DG. The accumulation of the CNBP signals in the myofiber membrane region suggested that CNBP might have a possible membrane function and prompted us to examine the interactions of CNBP with other proteins. To identify proteins interacting with CNBP, we used a recombinant CNBP protein fused with a maltose binding protein (MBP-CNBP). This protein was bound to amylose resin, and protein extracts from C2C12 and DM2 myotubes were incubated with MBP-CNBP. After intensive washing, proteins bound to MBP or MBP-CNBP were eluted with maltose and analyzed by gel electrophoresis. The staining of the eluted proteins showed that

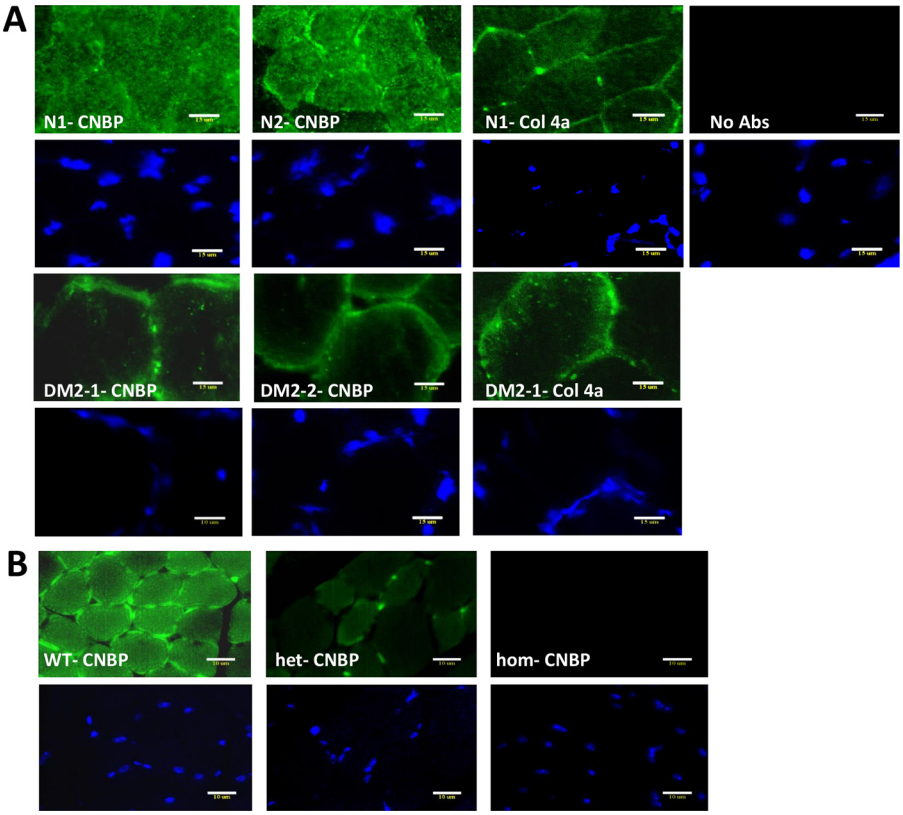

FIG 8 CNBP is reduced in cytoplasm of myofibers from human muscle biopsy specimens from patients with DM2. (A) IF analysis of CNBP in transverse muscle sections derived from two normal individuals (males, 45 and 50 years of age) with normal muscle histology and from two patients with DM2 (males, 43 and 44 years of age) was performed with antibodies to CNBP (8) with the same brightness and time of exposure, allowing quantification of the signals. Results of an IF assay with antibodies to the basement membrane protein collagen 4A (used as a control for membrane protein) are also shown, as are results from a negative IF assay lacking primary antibodies. Nuclear staining with DAPI (4′,6′-diamidino-2-phenylindole) is shown below each image. Scale bars, 15 μm. (B) IF analysis of Cnbp in skeletal muscle (gastrocnemius) of 1-month-old WT, het, and hom *Cnbp* KO mice with affinity-purified antipeptide antibodies to CNBP. Nuclei were stained with DAPI. Scale bars, 10 μm.

several proteins bind to MBP-CNBP in C2C12 myotubes (Fig. 9A). We found that among MBP-CNBP-bound proteins in DM2 myotubes there was a major protein with an approximate molecular mass of 156 kDa. A low-intensity protein band with the same mobility was also visible in the C2C12 pulldown proteins that interact with MBP-CNBP. We searched the literature for known muscle proteins with an approximate molecular mass of 150 kDa which might be located in the membrane and found that glycosylated α-dystroglycan (α-DG) migrates at a position corresponding to a protein with an approximate molecular mass of 156 kDa.

During studies of Duchenne muscular dystrophy (DMD), dystroglycans were identified as a part of a multimeric protein complex which contains dystrophin, sarcoglycans, sarcospan, dystropbrevin, and syntrophins (22). α-DG links to the extracellular matrix, whereas β-dystroglycan connects α-DG to the actin skeleton through dystrophin or utrophin.

To test whether the 156-kDa protein is α-DG, we analyzed the pulldown proteins from DM2 myotubes that interact with MBP-CNBP by Western blotting assay using antibodies to α-DG. This analysis showed that antibodies to α-DG recognize a protein with an approximate molecular mass of 156 kDa in MBP-CNBP pulldown samples from DM2 myotubes (Fig. 9B). Coimmunoprecipitation (co-IP) studies have shown that endogenous CNBP also interacts with α-DG in whole-cell protein extracts from normal and DM2 human muscle biopsy specimens and that this interaction is increased in

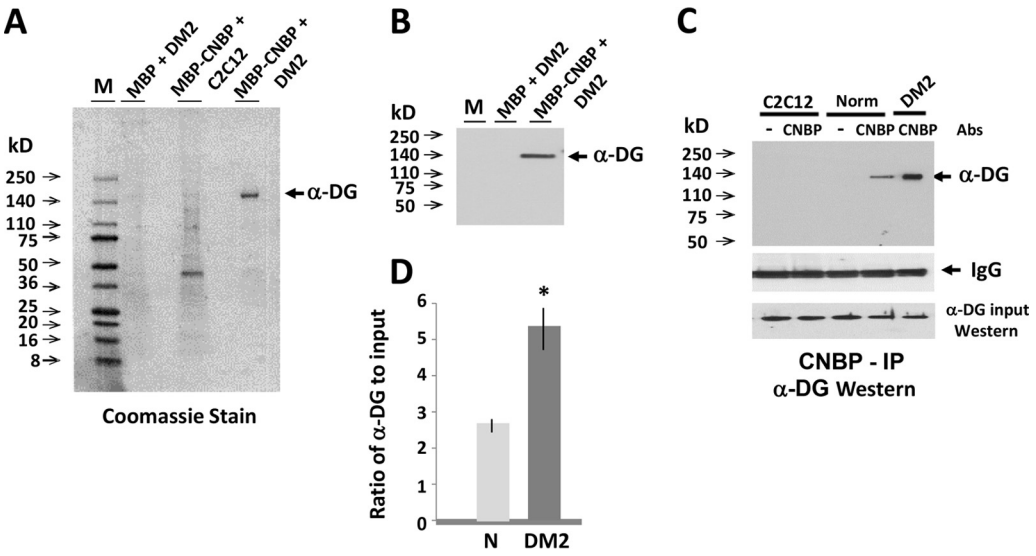

FIG 9 CNBP interacts with α-DG. (A) Electrophoretic analysis of C2C12 and DM2 proteins eluted from MBP or CNBP-MBP amylose. Amylose was incubated with whole-cell protein extracts from C2C12 and DM2 myotubes, with differentiation for 5 days. Eluted proteins were stained with Coomassie blue using a high-sensitivity protein detection protocol. A protein with an approximate molecular mass of 156 kDa bound to MBP-CNBP is shown by an arrow. Further immunological studies indicated that this protein is α-DG. (B) Western blot analysis of the pulldown samples from control resin, resin containing MBP, and resin containing MBP-CNBP incubated with whole-cell protein extracts from DM2 myotubes with antibodies to α-DG. The position of the immunoreactive band is shown by an arrow. (C) Endogenous CNBP binds to α-DG in human skeletal muscle. CNBP was immunoprecipitated from protein extract of C2C12 myotubes and protein extracts from human muscle biopsy specimens from normal control and DM2 patients with antibodies to CNBP. CNBP IPs were examined by Western blotting assay with antibodies to α-DG. Control immunoprecipitation was performed without primary antibodies. The IgG signal shows that equal amounts of antibodies to α-DG were added. The input signal (Western blotting) of α-DG shows the amounts of α-DG used in immunoprecipitation. (D) Quantification of the α-DG signals in the CNBP IPs from normal and DM2 muscle biopsy specimens (shown in panel C) as ratios to input signal. *, $P < 0.05$ for normal versus DM2 muscle.

skeletal muscle biopsy specimens from DM2 patients (Fig. 9C and D). These findings suggest that CNBP levels might be, at least partially, reduced in cytoplasm of DM2 muscle due to increased binding of CNBP to α-DG. Since α-DG is one of the components of the multimeric membrane complex DAPC, containing dystrophin and glycoproteins, it is possible that CNBP has increased interaction with DAPC in DM2. Figure 9A shows that several lower-molecular-mass proteins with reduced intensity relative to α-DG were detected in MBP-CNBP pulldown samples from C2C12 myotubes and to a lesser degree in pulldown samples from DM2 myotubes. Therefore, it is possible that, in addition to α-DG, CNBP interacts in DM2 with other proteins, including membrane proteins. Further studies are needed to determine whether these proteins represent other CNBP binding protein partners.

DISCUSSION

It has been shown that the pathogeneses of both DM1 and DM2 are associated with the disruption of RNA metabolism due to accumulation of toxic RNAs containing CUG and CCUG repeats (5). Despite phenotypic similarities between DM1 and DM2, there are distinct differences between these disorders, suggesting the involvement of an additional factor(s) in DM2. Our previous studies showed that the expanded CCUG repeats cause a cascade of toxic events in DM2 pathogenesis, including the reduction of cytoplasmic CNBP in skeletal muscle of patients with DM2 (8). These findings suggested that some symptoms in DM2 skeletal muscle might be associated with the reduction of CNBP.

In agreement, a previous study of adult het *Cnbp* KO mice showed that the reduction of Cnbp might disrupt skeletal and cardiac muscles, mimicking DM2 pathology (12). However, until now, the role of CNBP in DM2 has remained underappreciated because of (i) severe underdevelopmental defects (such as defects of the forehead) in

described *Cnbp* KO mice (19) and (ii) contradictory results on whether CNBP is truly reduced in muscle of patients with DM2 (8, 13–17). Gross analysis of *Cnbp* KO mice generated in our lab showed that although approximately half of hom *Cnbp* KO mice were not born or died after birth, the other half survived. hom survivors showed a delay of development, characterized by reduced size and weakness, but did not have obvious gross defects. het *Cnbp* KO mice did not show any gross developmental defects, as were observed in the previous study (19). Their muscle phenotype was very mild at a young age, but they developed a severe muscle wasting at an older age (Fig. 4D and E). They also showed grip weakness at all examined ages (Fig. 6A). Based on the analysis of our mouse model, we conclude that the reduction of Cnbp *in vivo* causes mild myopathy which is accompanied by weakness and leads to severe muscle atrophy at old age.

A complete loss of Cnbp causes a delay of neonatal myogenesis affecting sarcomere integrity. hom *Cnbp* KO survivors develop muscle atrophy at a young age. Fibers in hom *Cnbp* KO muscle are also variable in size and include both large and small atrophic fibers with centralized nuclei.

Protein analysis suggests that muscle atrophy in *Cnbp* KO mice may occur due to a reduction of translation of the TOP-mRNAs, putative targets of Cnbp. Since proteins encoded by the TOP-mRNAs regulate synthesis of muscle proteins, it is expected that the reduction of these proteins might cause the reduction of muscle mass.

Alterations of the regulators of muscle contractile proteins TNNT3, TPM2, and myosin regulatory light-chain 2 skeletal muscle isoform (MRLC) in *Cnbp* KO mice suggest that Cnbp might control muscle mRNAs with predicted Cnbp RNA binding sites (18). MRLC interacts with calcium ions and controls the structural integrity of myofiber. Reduction of MRLC in *Cnbp* KO muscle suggests that Cnbp may play a role in muscle contraction. TPM2 and TNNT3 are associated with the troponin complex and actin filaments. The increase of these proteins in muscle of *Cnbp* KO mice might be due to Cnbp-dependent misregulation of TPM2 and TNNT3 at the level of translation or transcription. It also might be a compensatory response to the deletion of Cnbp.

Muscle wasting in DM1 and DM2 may occur in combination with fat accumulation. DM2 is associated with insulin resistance and other metabolic changes. We found that the total body fat is increased and lean mass is reduced in het *Cnbp* KO mice. It remains to determine whether these changes are secondary response to the reduction of Cnbp or whether Cnbp function is associated with the regulation of metabolism.

Besides skeletal muscle, other tissues, such as cardiac muscle and CNS tissue, are affected in DM2. Therefore, it is critical to determine whether the Cnbp deficit in brain and heart in our *Cnbp* KO mice causes alterations reminiscent of the DM2 phenotype. We are investigating this issue, and our initial studies revealed underdevelopment of brain and heart in postnatal hom *Cnbp* KO mice (data not shown). Detailed analysis of these tissues in *Cnbp* KO mice of both genotypes is under way. We expect that a reduction of Cnbp in mice contributes to at least some defects in cardiac muscle and in the CNS.

One of the critical results of our study is that the intracellular distribution of CNBP is altered in mature fibers from patients with DM2. This result is in agreement with a report from R. Krahe's lab (14). The reduction of cytoplasmic CNBP in DM2 myofibers suggests that the cytoplasmic function of CNBP, associated with translation, is reduced in DM2. Interestingly, the CNBP signal is increased in the membranes of DM2 fibers (Fig. 8A). Our studies showed that CNBP interacts with a peripheral subunit of the membrane-spanning dystroglycan complex, α-DG, in DM2 muscle biopsy specimens (Fig. 9C and D). CNBP also interacts with α-DG in normal muscle, but this interaction is stronger in DM2 muscle (Fig. 9C and D). The dystroglycan complex is a core component of DAPC that is critical for protection of sarcolemma from the mechanical stress during muscle contraction. The increased binding of CNBP to α-DG in DM2 suggests that the function of α-DG and the DAPC complex might be affected in DM2 muscle.

What is the explanation for the fact that the CNBP protein with DNA and RNA binding activities is located on the fiber membrane? The existing knowledge demon-

strates that ZNF proteins are multifunctional. In addition to their binding to DNA and RNA, they function via interaction with other proteins and membrane association (23). For instance, the zinc finger domain FYVE, first identified in proteins Fab1p, YOTB, Vac1p, and early endosomal antigen 1 (EEA1), mediates the recruitment of proteins associated with membrane trafficking (24, 25). Therefore, it is possible that CNBP has several functions in skeletal muscle and in other tissues and that alteration of CNBP in DM2 cause muscle atrophy and weakness through reduction of CNBP in cytoplasm and through increased interactions of CNBP with membrane proteins affecting membrane functions. Although these mechanisms need to be determined, *in vivo* studies of our model of Cnbp and the previously described model show that CNBP may be considered a therapeutic target in DM2.

MATERIALS AND METHODS

***Cnbp* KO mouse model.** All animal experiments were approved by the IACUC at Baylor College of Medicine (BCM) and the Cincinnati Children's Hospital Medical Center (CCHMC). The ES clone, containing the gene trap insertion in the first intron of the *Cnbp* gene, from the Texas A&M Institute for Genomic Medicine (TIGM) (Houston, TX) was used to generate the *Cnbp* KO model in C57BL/6 mice in the TIGM facility. The gene trap vector contains two viral long terminal repeats (LTR) surrounding a *βgeo* sequence (fused *lacZ* and *neo*), which produces a β-galactosidase reporter and provides resistance to neomycin. The splice acceptor in the gene trap vector is located upstream of *βgeo*, and a phosphoglycerate kinase (PGK) promoter is located downstream of *βgeo*. The *Cnbp* insertion site was confirmed by sequencing.

For genotyping, the tail genomic DNA was extracted with the Kapa Express kit. The genotyping was performed using the following primers: 5′-CCAGGCACTTTCAGAGGAAG-3′ (forward), 5′-TCTCCAGAATTG GGTCAAGC-3′ (reverse), and 5′-CCAATAAACCCTCTTGCAGTTGC-3′ (downstream reverse). The PCR assay produced two products with the sizes 250 bp and 290 bp, corresponding to the WT and mutant Cnbp (Fig. 1B).

Grip strength analysis. The grip strength was determined as described previously (26, 27) using a grip strength meter (Columbus Instruments) in gender- and age-matched groups of WT, het, and hom *Cnbp* KO mice at 1, 3, 6, and 12 months.

Muscle histology and EM. Skeletal muscle histology was examined in gastroc and soleus of the age- and gender-matched mice. Paraffin sections were stained with H&E in the Pathology Core facilities of BCM and CCHMC. The average fiber area, the number of central nuclei, and the number of fibers in the gastroc were determined from the matched WT and *Cnbp* KO mice using the MetaMorph (Molecular Devices) software as described previously (26, 27). For the examination of the average fiber area, 600 to 1,300, 1,000 to 2,200, and 900 to 1,700 fibers were examined in the gastroc from 1-, 4-, and 16-month-old WT, het, and hom *Cnbp* KO mice, respectively. Since the gastroc weight of hom *Cnbp* KO mice is reduced relative to that of WT mice, the measurements of the average fiber area in WT and hom muscles were corrected to the muscle weight.

The average number of central nuclei was determined by counting central nuclei in the matched gastroc in random areas at a magnification of ×20 in gender (male)- and age-matched WT and hom *Cnbp* KO mice.

The total number of fibers in the matched gastrocs of WT and hom mice was determined by counting fibers in random locations of similar muscle areas at a magnification of ×20. The counts of the fiber number in WT and hom mice were corrected to adjust to the reduction of gastroc weight in hom mice relative to WT mice.

For the EM analysis, the entire fresh hind limbs of 1-day-old WT and hom *Cnbp* KO mice were sequentially fixed in 4% formaldehyde and in 3% glutaraldehyde supplemented with 0.4% tannic acid and analyzed in the Pathology Core of CCHMC as described previously (26). Fixed muscle samples were postfixed in 1% osmium tetroxide for 1 h at 4°C, counterstained with 1% uranyl acetate for 2 h, and infused with epoxy resin. The quality of muscle sections was verified by light microscopy after staining with 1% toluidine blue O. Ultrathin sections (50 to 70 nm) were stained with uranyl acetate and Sato lead stain and analyzed using a Hitachi transmission electron microscope (model H-7650). The number of myofibrils was counted in 49 images in WT muscle and in 82 images in hom *Cnbp* KO muscle at a magnification of ×30,000. The numbers of the analyzed sarcomeres were 286 (WT muscle) and 233 (*Cnbp* KO muscle).

The integrity of the I bands was analyzed in 286 sarcomeres in WT muscle and in 233 sarcomeres in hom *Cnbp* KO muscle. To determine the percentage of intact I bands, the number of all counted I bands, including intact and disrupted I bands in each muscle, was set at 100%.

Immunoanalysis. Mouse skeletal or cardiac muscle samples were homogenized in radioimmunoprecipitation assay (RIPA) buffer. Western blot analysis was performed as described previously (8) using antibodies to RPS17, PABPC1, TNNT3, TPM2, and α-DG from Santa Cruz Biotechnologies, actin (Sigma-Aldrich), affinity-purified antibodies to CNBP (8), or goat antibodies to CNBP from Abcam. IF analysis of human muscle sections was performed with affinity-purified rabbit Abs to CNBP (8) and with goat anti-CNBP from Abcam according to the manufacturer's protocol. An IF assay lacking primary Abs was used as a negative control. As a control for membrane staining, IF with antibodies to collagen 4A (Abcam) was used. The images of human muscle sections from three healthy control persons with normal histopathology and four patients with DM2 were analyzed using a Nikon microscope with the same time

of exposure and the same brightness. CNBP and α-DG co-IP experiments were performed using total protein extracts from human muscle biopsy specimens as described previously (26). The use of human muscle samples was according to the Human Subjects Protocol, approved by the Institutional Review Board at Baylor College of Medicine. The use of human samples without direct interactions with patients is considered not to be human subject research at CCHMC and did not require a human subject protocol.

2D gel separation and mass spectroscopy analysis. Total muscle proteins extracted from soleus of 3-month-old WT and hom *Cnbp* KO mice (males, three mice per genotype) were labeled with fluorescent dyes at Applied Biomics (Hayward, CA). Proteins were separated by isoelectrofocusing and SDS-gel electrophoresis. Three pair of gels containing proteins from WT and *Cnbp* KO muscles were scanned using a Typhoon scanner, and the intensities of the spots were compared for each pair of WT and *Cnbp* KO muscles. As an internal standard, a mix of equal portions of all 6 protein samples was labeled with Cy2 and separated by 2D gel electrophoresis. Approximately 3,300 spots were identified on each gel. The volume of each spot was determined, and the standard deviations based on three repeats were deduced. The numbers of spots with increased and reduced levels in *Cnbp* KO muscle were determined. A total of 79 spots with altered expression were identified. The *P* values were calculated based on the ratios between signals in WT and *Cnbp* KO muscle using three pairs of gels. Fifty-eight spots showed *P* values of <0.05. Fourteen protein spots, including 10 well-separated spots from *Cnbp* KO muscle and four positive-control spots (β-galactosidase), were subjected to initial mass spectroscopy. These protein spots were gel cleaned and digested with trypsin, and peptides were extracted. After desalting, the peptides were subjected to tandem matrix-assisted laser desorption ionization–time of flight (MALDI-TOF/TOF) analysis. The identified sequences were analyzed using the NCBI or Swiss-Prot database. Twelve proteins, including four positive controls, showed high protein scores, suggesting high confidence for the results. The protein spot for cofilin 2 showed a low score (54%). The spot for Hsp70 showed possible contaminations for annexin A6 and myosin 4, and the spot for microphthalmia-associated transcription factor (MITF) showed possible contaminations with fragments of other large proteins.

CNBP protein interaction. A recombinant human CNBP fused in frame with maltose binding protein (MBP-CNBP) was attached to amylose resin. Total protein extracts was prepared from C2C12 and human DM2 myotubes grown for 5 days in fusion medium as previously described (27). Two hundred to 300 μg of protein extracts was loaded on the amylose column bound with MBP or MBP-CNBP. The column was intensively washed with the loading buffer, and bound proteins were eluted with 10 mM maltose. Eluted proteins were analyzed by polyacrylamide gel electrophoresis and subjected to high-sensitivity staining with Coomassie blue (28).

Statistical analysis. Protein signals in the Western blot assay were determined by scanning densitometry relative to control protein (β-actin), and mean data based on three repeats are presented. Statistical analysis was performed using a two-tailed Student *t* test. Comparison between three groups of mice was performed by analysis of variance (ANOVA). A *P* value of <0.05 was considered statistically significant. The ratio of expected and observed results for WT, het, and hom mice was examined by Fisher's exact test.

ACKNOWLEDGMENTS

We are grateful to Luke Turner for the initial experiments with the muscle histology.

This work was supported by NIH grants AR052791 and AR064488 (L.T.) and CA159942 and DK102597 (N.A.T.) and by Internal Development Funds from CCHMC (L.T. and N.A.T.).

The funders had no role in study design, data collection and interpretation, or the decision to submit the work for publication.

The experiments were designed by L.T. C.W. and L.S. carried out experimental work. C.S.-G. and C.S. provided reagents. C.W., C.S.-G., N.A.T., and L.T. analyzed data and prepared the manuscript.

REFERENCES

1. Day JW, Ricker K, Jacobsen JF, Rasmussen LJ, Dick KA, Kress W, Schneider C, Koch MC, Beilman GJ, Harrison AR, Dalton JC, Ranum LP. 2003. Myotonic dystrophy type 2: molecular, diagnostic and clinical spectrum. Neurology 60:657–664. https://doi.org/10.1212/01.WNL.0000054481.84978.F9.
2. Liquori CL, Ricker K, Moseley ML, Jacobsen JF, Kress W, Naylor SL, Day JW, Ranum LP. 2001. Myotonic dystrophy type 2 caused by a CCTG expansion in intron 1 of ZNF9. Science 293:864–867. https://doi.org/10.1126/science.1062125.
3. Fu YH, Pizzuti A, Fenwick RG, Jr, King J, Rajnarayan S, Dunne PW, Dubel J, Nasser GA, Ashizawa T, de Jong P, Wieringa B, Korneluk R, Perryman MB, Epstein HF, Caskey CT. 1992. An unstable triplet repeat in a gene related to myotonic muscular dystrophy. Science 255:1256–1258. https://doi.org/10.1126/science.1546326.
4. Vihola A, Bassez G, Meola G, Zhang S, Haapasalo H, Paetau A, Mancinelli E, Rouche A, Hogrel JY, Laforêt P, Maisonobe T, Pellissier JF, Krahe R, Eymard B, Udd B. 2003. Histopathological differences of myotonic dystrophy type 1 (DM1) and PROMM/DM2. Neurology 60:1854–1857. https://doi.org/10.1212/01.WNL.0000065898.61358.09.
5. Schoser B, Timchenko L. 2010. Myotonic dystrophies 1 and 2: complex diseases with complex mechanisms. Curr Genomics 11:77–90. https://doi.org/10.2174/138920210790886844.
6. Mateos-Aierdi AJ, Goicoechea M, Aiastui A, Fernández-Torrón R, Garcia-Puga M, Matheu A, López de Munain A. 2015. Muscle wasting in myotonic dystrophies: a model of premature aging. Front Aging Neurosci 7:125. https://doi.org/10.3389/fnagi.2015.00125.
7. Calcaterra NB, Armas P, Weiner AM, Borgognone M. 2010. CNBP: a multifunctional nucleic acid chaperone involved in cell death and proliferation control. IUBMB Life 62:707–714. https://doi.org/10.1002/iub.379.

8. Huichalaf C, Schoser B, Schneider-Gold C, Jin B, Sarkar P, Timchenko L. 2009. Reduction of the rate of protein translation in patients with myotonic dystrophy 2. J Neurosci 29:9042–9049. https://doi.org/10.1523/JNEUROSCI.1983-09.2009.
9. Pellizzoni L, Lotti F, Maras B, Pierandrei-Amaldi P. 1997. Cellular nucleic acid binding protein binds a conserved region of the 5′ UTR of Xenopus laevis ribosomal protein mRNAs. J Mol Biol 267:264–275. https://doi.org/10.1006/jmbi.1996.0888.
10. Rojas M, Farr GW, Fernandez CF, Lauden L, McCormack JC, Wolin SL. 2012. Yeast Gis2 and its human ortholog CNBP are novel components of stress-induced RNP granules. PLoS One 7:e52824. https://doi.org/10.1371/journal.pone.0052824.
11. Benhalevy D, Gupta SK, Danan CH, Ghosal S, Sun H-W, Kazemier HG, Paeschke K, Hafner M, Juranek SA. 2017. The human CCHC-type zinc finger nucleic acid binding protein binds G-rich elements in target mRNA coding sequences and promotes translation. Cell Rep 18:2979–2990. https://doi.org/10.1016/j.celrep.2017.02.080.
12. Chen W, Wang Y, Abe Y, Cheney L, Udd B, Li YP. 2007. Haploinsufficiency for ZNF9 in ZNF9+/− mice is associated with multiorgan abnormalities resembling myotonic dystrophy. J Mol Biol 368:8–17. https://doi.org/10.1016/j.jmb.2007.01.088.
13. Pelletier R, Hamel F, Beaulieu D, Patry L, Haineault C, Tarnopolsky M, Schoser B, Puymirat J. 2009. Absence of a differentiation defect in muscle satellite cells from DM2 patients. Neurobiol Dis 36:181–190. https://doi.org/10.1016/j.nbd.2009.07.009.
14. Raheem O, Olufemi SE, Bachinski LL, Vihola A, Sirito M, Holmlund-Hampf J, Haapasalo H, Li YP, Udd B, Krahe R. 2010. Mutant (CCTG)n expansion causes abnormal expression of zinc finger protein 9 (ZNF9) in myotonic dystrophy type 2. Am J Pathol 177:3025–3036. https://doi.org/10.2353/ajpath.2010.100179.
15. Botta A, Caldarola S, Vallo L, Bonifazi E, Fruci D, Gullotta F, Massa R, Novelli G, Loreni F. 2006. Effect of the [CCTG]n repeat expansion on ZNF9 expression in myotonic dystrophy type II (DM2). Biochim Biophys Acta 1762:329–334. https://doi.org/10.1016/j.bbadis.2005.11.004.
16. Margolis JM, Schoser BG, Moseley ML, Day JW, Ranum LP. 2006. DM2 intronic expansions: evidence for CCUG accumulation without flanking sequence or effects on ZNF9 mRNA processing or protein expression. Hum Mol Genet 15:1808–1815. https://doi.org/10.1093/hmg/ddl103.
17. Massa R, Panico MB, Caldarola S, Fusco FR, Sabatelli P, Terracciano C, Botta A, Novelli G, Bernardi G, Loreni F. 2010. The myotonic dystrophy type 2 (DM2) gene product zinc finger protein 9 (ZNF9) is associated with sarcomeres and normally localized in DM2 patients' muscles. Neuropathol Appl Neurobiol 36:275–284. https://doi.org/10.1111/j.1365-2990.2010.01068.x.
18. Scherrer T, Femmer C, Schiess R, Aebersold R, Gerber AP. 2011. Defining potentially conserved RNA regulons of homologous zinc-finger RNA-binding proteins. Genome Biol 12:R3. https://doi.org/10.1186/gb-2011-12-1-r3.
19. Chen W, Liang Y, Deng W, Shimizu K, Ashique AM, Li E, Li Y-P. 2003. The zinc-finger protein CNBP is required for forebrain formation in the mouse. Development 130:1367–1379. https://doi.org/10.1242/dev.00349.
20. Schoser BG, Schneider-Gold C, Kress W, Goebel HH, Reilich P, Koch MC, Pongratz DE, Toyka KV, Lochmüller H, Ricker K. 2004. Muscle pathology in 57 patients with myotonic dystrophy type 2. Muscle Nerve 29:275–281. https://doi.org/10.1002/mus.10545.
21. Salisbury E, Schoser B, Schneider-Gold C, Wang GL, Huichalaf C, Jin B, Sirito M, Sarkar P, Krahe R, Timchenko NA, Timchenko LT. 2009. Expression of RNA CCUG repeats dysregulates translation and degradation of proteins in myotonic dystrophy 2 patients. Am J Pathol 175:748–762. https://doi.org/10.2353/ajpath.2009.090047.
22. Winder SJ. 2001. The complexities of dystroglycan. Trends Biochem Sci 26:118–124. https://doi.org/10.1016/S0968-0004(00)01731-X.
23. Laity JH, Lee BM, Wright PE. 2001. Zinc finger proteins: new insights into structural and functional diversity. Curr Opin Struct Biol 11:39–46. https://doi.org/10.1016/S0959-440X(00)00167-6.
24. Stahelin RV, Long F, Diraviyam K, Bruzik KS, Murray D, Cho W. 2002. Phosphatidylinositol 3-phosphate induces the membrane penetration of the FYVE domains of Vps27p and Hrs. J Biol Chem, 277:26379–26388. https://doi.org/10.1074/jbc.M201106200.
25. Misra S, Hurley JH. 1999. Crystal structure of phosphatidylinositol 3-phosphate-specific membrane-targeting motif, the FYVE domain of Vps27p. Cell 97:657–666. https://doi.org/10.1016/S0092-8674(00)80776-X.
26. Jones K, Wei C, Iakova P, Bugiardini E, Schneider-Gold C, Meola G, Woodgett J, Killian J, Timchenko NA, Timchenko LT. 2012. GSK3β mediates muscle pathology in myotonic dystrophy. J Clin Invest 122:4461–4472. https://doi.org/10.1172/JCI64081.
27. Wei C, Stock L, Valanejad L, Zalewski ZA, Karns R, Puymirat J, Nelson D, Witte D, Woodgett J, Timchenko NA, Timchenko L. 2018. Correction of GSK3β at young age prevents muscle pathology in mice with myotonic dystrophy type 1. FASEB J 32:2073–2085. https://doi.org/10.1096/fj.201700700R.
28. Gauci VG, Padula MP, Coorssen JR. 2013. Coomassie blue staining for high sensitivity gel-based proteomics. J Proteomics 90:96–106. https://doi.org/10.1016/j.jprot.2013.01.027.